Dyes and Pigments 87 (2010) 119–124

Contents lists available at ScienceDirect

Dyes and Pigments

journal homepage: www.elsevier.com/locate/dyepig

The preparation and TD-DFT studies of 1-[(4-methyl-2-nitrophenyl) azo]-2-naphthalenol (C.I. Pigment Red 3) nanoparticles

Yuan Le [a,*], Wuwei An [a], Jian-Feng Chen [b,*]

[a] Key Lab for Nanomaterials, Ministry of Education, Beijing University of Chemical Technology, Beijing 100029, PR China
[b] Research Center of the Ministry of Education for High Gravity Engineering and Technology, Beijing University of Chemical Technology, Beijing 100029, PR China

ARTICLE INFO

Article history:
Received 28 December 2009
Received in revised form
3 March 2010
Accepted 4 March 2010
Available online 12 March 2010

Keywords:
1-[(4-methyl-2-nitrophenyl)azo]-2-naphthalenol
Nanoparticles
Electrophoresis
Conformers
Electronic transition
UV–vis spectra

ABSTRACT

Nanosized 1-[(4-methyl-2-nitrophenyl)azo]-2-naphthalenol (C.I. Pigment Red 3) particles were prepared using a facile liquid precipitation method. The morphology and electrical properties of the produced particles were characterized by SEM, ζ-potential and electrophoretic display device. The particles were ~80 nm in size within a narrow particle size distribution and displayed excellent electrophoretic properties. The structure and geometry of 1-[(4-methyl-2-nitrophenyl)azo]-2-naphthalenol were investigated using density functional theory, for which, calculated results indicated that the compound possessed both trans- and cis- conformers. UV–vis spectroscopy of the two conformers was evaluated using time-dependent density functional theory taking bulk solvent effects into account by means of the polarizable continuum model. Vertical excitation energies and oscillator strengths were determined for the lowest-energy electronic transitions. The calculated results reproduced the experimental data and corroborated the reliability of the structural characterization of the pigment.

1. Introduction

Electrophoresis is the movement of charged pigment particles, suspended in a medium (organic solvents), under the influence of an electric field. Since the late 1990s, the development of electrophoretic image displays (EPIDS) has made much progress in the search for low-cost, flexible, electronic displays [1–4]. In an electrophoretic display, the particles are required to migrate repeatedly between electrodes by changing the polarity of the applied field, without adhering to the electrode surface, depositing or changing electrostatic properties. The characteristics of electrophoretic particles are the key factor in determining image quality; the most important criteria are particles size, scattering properties and density [5]. Generally, many kinds of dyes and pigments can be used as electrophoretic particles. Recent research has focused on inorganic pigments and polymeric particles such as TiO_2 [6–8], CdS [9], black particles of P(MMA-co-EGDMA) [10] and acrylic-based oil blue N [11].

Currently, black–white electronic books based on EPIDS have been commercialized and, with color displays being a further target, the screening of suitable coloured particles for EPIDS is attractive. The purposes of this work were to adopt a simple routine to prepare spherical, colored particles with good electrophoretic properties and to study the structure and properties of the particles using quantum chemical calculations.

Compared with inorganic pigments, organic compounds are much more diverse and offer great potential in the context of electronic, optical and photoelectric devices [12–14]. The red pigment 1-[(4-methyl-2-nitrophenyl)azo]-2-naphthalenol (C.I. Pigment Red 3; *toluidine red*, TR) has enjoyed widespread usage because of its bright scarlet hue, high tinctorial strength and good stability to acids, alkalis and light. C.I. Pigment Red 3 has been used in paints, printing inks and paper coatings. Owing to its good light scattering properties and density similar to that of common organic suspending media, the pigment offers potential as an electrophoretic particulate material.

C.I. Pigment Red 3 is an azo compound, which are known to have stable trans- and cis- conformers [15–17]. Although the crystalline structure of TR has been determined by X-ray diffraction [18], the trans- and cis- conformers have not been determined experimentally. Thus, it was decided to obtain the accurate structure of TR for investigating associated optical properties; in addition, knowledge

* Corresponding authors. Tel.: +86 10 64447274; fax: +86 10 64423474.
E-mail addresses: leyuan@mail.buct.edu.cn (Y. Le), chenjf@mail.buct.edu.cn (J.-F. Chen).

0143-7208/$ – see front matter © 2010 Elsevier Ltd. All rights reserved.
doi:10.1016/j.dyepig.2010.03.005

of the pigment's structure is an essential prerequisite for understanding its properties and reactivity, especially the way in which its structure is modified by different solvents and solid environments.

Trans- and cis- isomerization is induced by the electronic excitation of an electron from either the highest occupied nonbonded orbital or the highest occupied orbital to the lowest unoccupied orbital. Excited states are directly involved in the primary steps of light absorption and charge-transfer. Understanding excited states and how their characteristics depend on chemical environment is of great interest for technological applications.

Although a large number of experimental data are available for azo dyes [19], it is difficult to secure a systematic picture of how different combinations of functional groups at various positions within azo colorants affect excitation energy. To our knowledge, few experimental and theoretical reports exist on the equilibrium geometry and vertical excitation energies of trans- and cis-TR.

In this work, C.I. Pigment Red 3 nanoparticles were prepared using a liquid precipitation rout and were characterized by SEM and an EPID device. The stable geometry of TR were optimized using DFT employing the B3LYP/6-31 + G* level. Experimental UV–vis spectra were interpreted with the help of TD-DFT quantum chemical calculations and bulk solvent effects on singlet vertical excited states were surveyed using the polarized continuum model (PCM) method [20–22].

2. Experimental and computational details

2.1. Preparation of TR nanoparticles

C.I. Pigment Red 3 crude powder (5–10 μm) was purchased from Qianmen Chemical, China. Tetrachloroethylene (C_2Cl_4) was purchased from Guangdong Xilong chemical factory. Concentrated H_2SO_4 and isopropyl alcohol were obtained from Beijing chemical factory, China. Alkyl hydroxy oximido acid (AHOA) was purchased from China University of mining and technology. All chemicals were reagent grade and used as purchased without further purification.

TR nanoparticles were prepared using an anti-solvent precipitation method. In a typical experiment, 0.03 g TR was dissolved in 5 mL concentrated H_2SO_4 (solvent). 0.375 g modifier AHOA was dissolved in 2 mL isopropyl alcohol, and then AHOA solution was poured rapidly into 100 mL deionized water (anti-solvent) with stirring. Subsequently, 5 mL pigment solution was added dropwise to the anti-solvent at 298 K with stirring; the volume ratio of solvent:anti-solvent was1:20. The system became turbid immediately and a suspension formed, indicating the onset of precipitation. After stirring for 20 s, 10 mL C_2Cl_4 was added as extractant. Finally, the TR–C_2Cl_4 suspension was obtained.

2.2. Characterization

Scanning Electron Microscopy (SEM, JSM-6360LV) specimens were prepared by placing a drop of the final suspension on a piece of cover glass. The drop was dried in air at room temperature and then sputter-coated under vacuum with a thin layer of gold.

UV–vis spectra were obtained in carbon tetrachloride (CCl_4), ethanol (EtOH) and dimethylsulfoxide (DMSO) solutions which performed on Shimadzu UV-2501PC.

ζ-potential was measured by means of a Malvern 3000HS Zetasizer. 1.5 mL suspension of the prepared particles dispersed in C_2Cl_4 was pipetted into a disposable cuvette. Then plug the electrode into cuvette. The ζ-potential for one sample was run from 3 times.

Sedimentation ratio is often used as the simplest semi-quantitative technique available for rating the stability of a concentrated dispersion [5]. Sedimentation ratio is the ratio of the volume of clear liquid to the volume of the original suspension. In this experiment, TR–C_2Cl_4 suspension was sonified and placed in a i.d. glass tube with measurement. The ratio of settling was recorded visually from beginning to some days storage at room temperature.

Electronic ink with C_2Cl_4 as medium was prepared in the presence of white dyes. It was then introduced in an electrophoretic cell, composed of two ITO-covered glass slides with 300 μm gap space. Finally, 100 mV/μm DC electric field was applied to the cell. Response time of the particles in electric field was measured by self-made EPID instrument.

2.3. Computational methods

The optimized geometries of TR were computed by density functional theory using B3LYP with 6-31 + G* basis set. Full geometry optimizations of a single molecule were carried out without symmetry constraints. Consequently, PCM was used for evaluating the bulk solvent effects, in which one divides the problem into a solute part (TR) lying inside a cavity and a solvent part (in our case, CCl_4, EtOH and DMSO) represented as a structureless material, characterized by its dielectric constant as well as other parameters [23]. Geometry vibrational frequencies were calculated analytically to ensure it to be a true local minimum (no imaginary frequencies). Vertical electronic excitation processes were studied by using time-dependent DFT approach [24–26] which is proved to be a powerful and effective computational tool for the study of ground and excited state properties by comparison to the available experimental data [27,28]. 10 lowest-energy electronic excited states were computed for all the molecules. TDDFT calculations were carried out using the B3LYP/6-31 + G* on the previously optimized molecular geometries obtained at the same

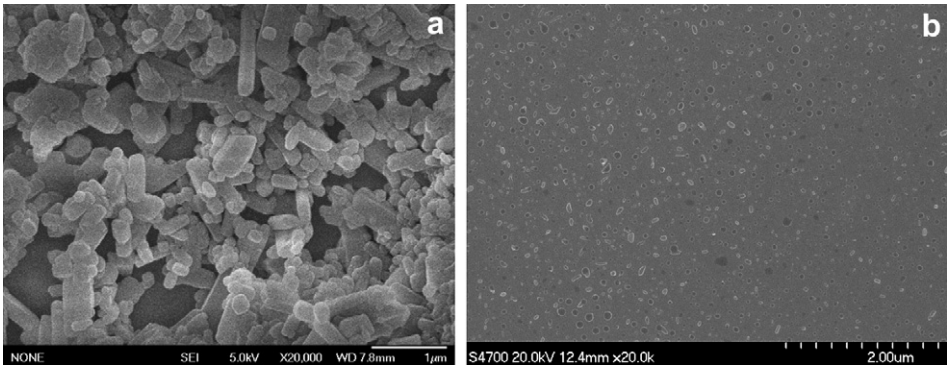

Fig. 1. SEM images of TR (a) crude powder (b) nanoparticles.

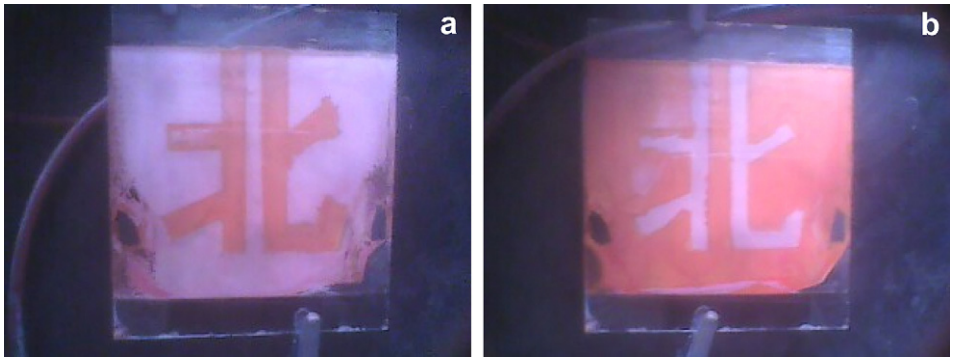

Fig. 2. Electrophoretic display in the electric field ($E = 100$ V/mm), (a) positive field is applied to the upper plate, (b) negative field is applied to the upper plate.

level of calculation. All calculations were performed using Gaussian 03 package on the Intel Pentium IV PC.

3. Results and discussion

3.1. Characterization of TR nanoparticles

SEM images of TR crude and nanosized particles are shown in Fig. 1. It can be seen that the prepared TR is uniform spherical particles with average size of 80 nm, while the crude TR shows irregular shape of 750 nm in size with wide particle size distribution. Evidently, the prepared TR particles are significantly smaller and more uniform than crude TR, which should be more beneficial for enhancing resolution and performance of electrophoretic display. In comparison, ζ-potential of the TR nanoparticles is −53.6 mV, much higher than 0 mV of crude powder. Besides, sedimentation ratio of the TR nanoparticles in C_2Cl_4 is nearly down to 15% within 100 h compared to that of 96% for raw materials. Experimental results illustrate the prepared TR nanoparticles are suitable for electrophoretic display.

Fig. 2 exhibits a response behavior of the TR nanoparticles in electrophoretic display. Controlling voltage applied to the electrodes enables images to be displayed. When positive DC electric field ($E = 100$ V/mm) is applied to the upper plate, TR particles filled in the pattern migrate fast to the upward (Fig. 2(a)), then the image shows red color. While the DC electric field is revised, the white dyes come to the upper plate and red particles are pulled back acting as background (Fig. 2(b)), with a response time of 2 s. The stationary image can be kept about 10 min after the electric field is removed.

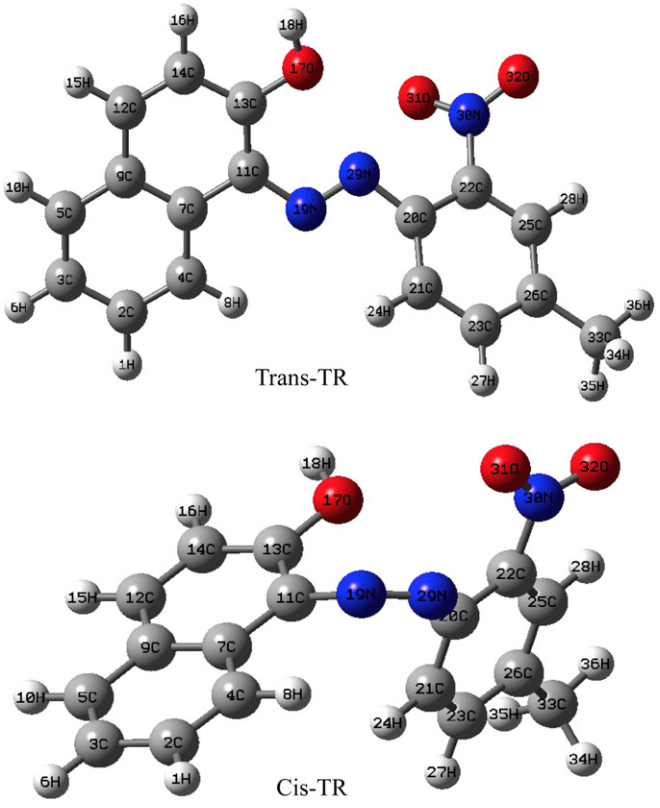

Fig. 3. Optimized structure of TR determined at the B3LYP/6-31 + G* level.

3.2. Ttrans- and cis- conformers

The crystalline structure of TR has been characterized as a monoclinic symmetry using XRD [18]. The rigid bonds of the phenyl ring and naphthyl ring do not provide any internal rotation. Different conformers of TR molecule result from rotating the main two axes of C–N bonds, then the conformational structure of TR molecule can be characterized with relevant torsion angles $C_7–C_{11}–N_{19}–N_{29}$ and $C_{22}–C_{20}–N_{19}–N_{29}$. After local minima optimization, the two lowest-energy conformers–trans-TR and cis-TR correspond to the noticeable changes of geometric structures are

Table 1
Geometry parameters of TR calculated by B3LYP/6-31 + G*.

Structure parameters	Trans	Cis
Bond length (Å)		
$N_{19}–N_{29}$	1.2620	1.2468
$C_{11}–N_{19}$	1.4000	1.4281
$N_{29}–C_{20}$	1.4128	1.4223
$C_{13}–O_{17}$	1.3564	1.3643
$C_{22}–N_{30}$	1.4699	1.4671
Bond angle (°)		
$C_7–C_{11}–N_{19}$	114.88	115.67
$C_{11}–N_{19}–N_{29}$	117.65	124.48
$N_{19}–N_{29}–C_{20}$	113.80	123.84
$C_{22}–C_{20}–N_{29}$	119.48	122.52
Torsion angle (°)		
$C_7–C_{11}–N_{19}–N_{29}$	164.08	137.58
$C_{22}–C_{20}–N_{19}–N_{29}$	155.26	135.35
$C_{11}–N_{19}–N_{29}–C_{20}$	174.90	−12.12
E (hartree)	−1045.4626	−1045.4461
ΔE (kJ mol^{-1})		43.32
μ(D)	4.623	7.791
ΔE_{gap} (eV)	3.230	3.216

Table 2
Calculated solvent energies, dipole moments and frontier orbital energies.

Conformer	Trans-TR			Cis-TR		
Solvent	CCl_4	EtOH	DMSO	CCl_4	EtOH	DMSO
E_s(kJ mol$^{-1)}$	30.45	74.30	76.40	33.87	82.70	85.07
ΔE_{gap} (eV)	3.216	3.192	3.181	3.214	3.140	3.132
μ(D)	5.284	6.173	6.225	9.083	11.053	11.191

depicted in Fig. 3. The selected calculated bond length, bond angles and important torsion angles of TR conformers are given in Table 1.

The most remarkable difference between trans- and cis-TR is the C–N–N–C dihedral angle which is the twist angle between the phenyl ring and the naphthyl ring around the C–N=N–C plane. It is obvious that trans-TR shows nearly planar structure, value of C_{11}–N_{19}–N_{29}–C_{20} is 174.90°. Whereas cis-TR is completely nonplanar, the value of C_{11}–N_{19}–N_{29}–C_{20} is −12.12°. Because the π electrons of cis-TR prefer to localized on the N=N bond compared to the large π-conjugation in trans-TR, it is expected that the N=N bond in cis-TR is shorter than that in trans and that the C–N bonds in cis-TR are longer than that in trans, which have been proved by the calculated results. The N=N bond length of trans-TR is 1.2620 Å, longer than that (1.2468 Å) of cis-TR, whereas C–N distance of trans-TR (C_{11}–N_{19} = 1.4000 Å, N_{29}–C_{20} = 1.4128 Å) are shorter than those (1.4281 Å and1.4223 Å) of cis-TR. The total energies and relative stability of trans-TR and cis-TR are also presented in Table 1. The trans-TR is 43.32 kJ/mol more stable than cis-TR in vacuum. Furthermore, the trans- and cis- TR have different dipole moments. The cis- TR values 3.17 D higher than that of the trans- TR.

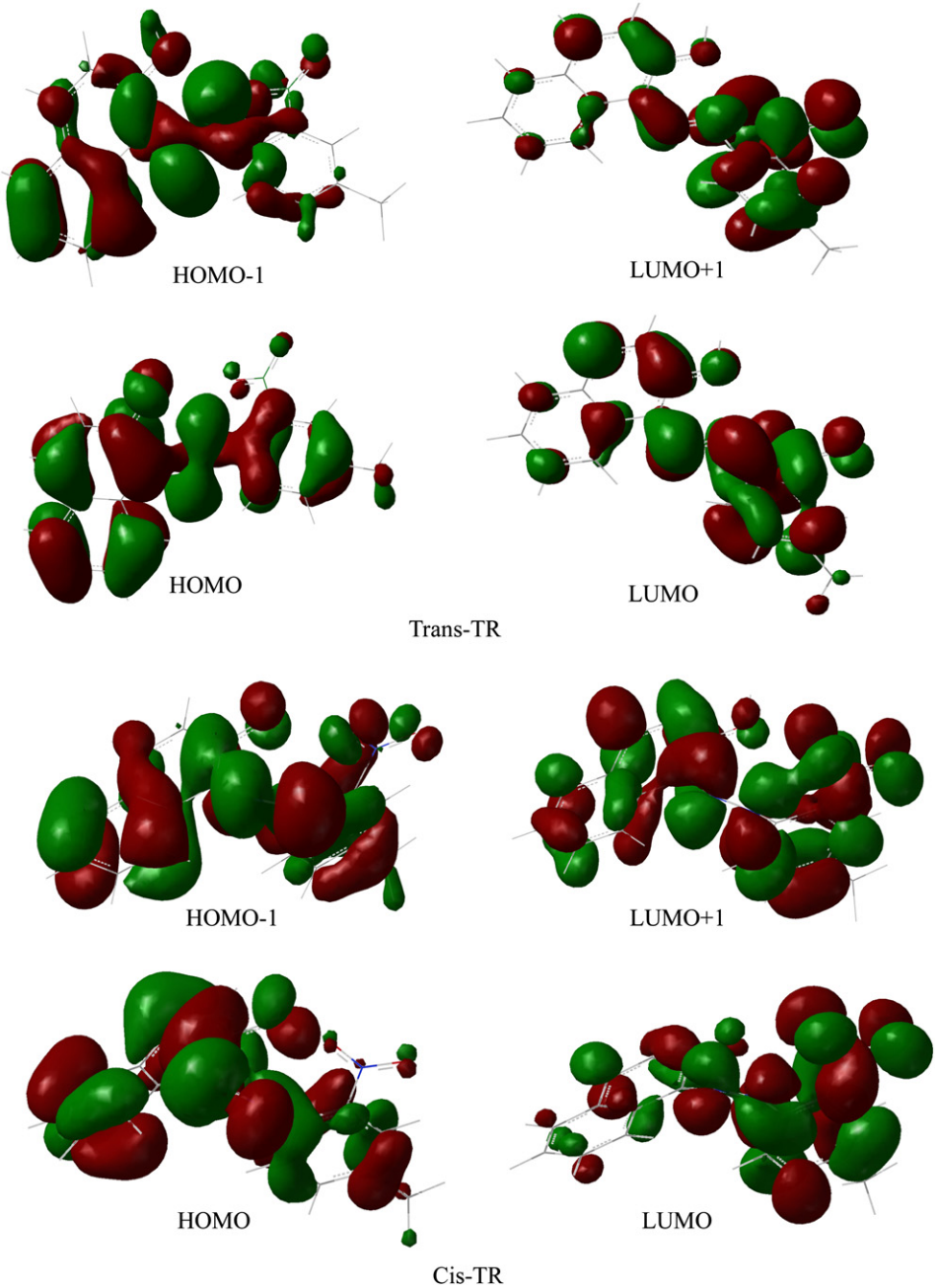

Fig. 4. Plots of the molecular orbitals of trans and cis TR from the calculations.

The calculated solvent energies (E_S), frontier orbital energies and dipole moments of the two conformers in solutions are listed in Table 2. With the increase of solvent dielectric constant, the energy gap (ΔE_{gap}) between the highest occupied molecular orbital (HOMO) and the lowest unoccupied molecular orbital (LUMO) slightly decrease while solvent energies and dipole moments enhance. UV absorption wavelength versus the ΔE_{gap}, so that the wavelength is predicted increasing with the increase of dielectric constant. Solvent effects improve the charge delocalized in the molecules, therefore, induce the dipole moments raising, furthermore, solvent energies show correlation with the dielectric constant or dipole moment. From Table 2, it can be seen that the difference of ΔE_{gap} between trans- and cis- TR are limit, only 0.014 eV.

3.3. UV-vis spectra

TR molecule formed by a naphthyl ring and a phenyl ring connected by azo linkage, has some interacting chromophoric groups that generate a crowd of closely spaced excited states. From a qualitative standpoint, the main electronic excitations of TR should bear $n \rightarrow \pi^*$ and $\pi \rightarrow \pi^*$ character. However, as a results of a complex balance of through-bond and through-space bone interactions, the various n (N, O) semilocalized orbitals are significantly mixed and the π orbitals are not restricted within a single ring but spread over the entire molecular skeleton [29]. Fig. 4 shows the topologies of the first two frontier MOs of trans- and cis-TR. As expected, all the frontier orbitals show π characters. Both the HOMO and the HOMO-1 are bonding across the full molecular skeleton. Conversely, the LUMO and the LUMO + 1 are antibonding, mainly occupy phenyl ring. The two orbitals within both occupied and vacant pairs are relatively close in energy, for trans-TR, with deviation of 0.45 eV and 0.52 eV, for cis-TR, with separations of 0.62 eV and 0.55 eV respectively. From these calculations, it also becomes apparent that the HOMO and LUMO topologies and sizes are similar for the two conformers.

To provide insight into the nature of the UV–vis absorptions observed experimentally for the TR, the lowest-energy electronic excited states in different solvents were calculated using TDDFT approach on the previously optimized ground-state molecular geometry of the two conformers. Experimental and theoretical λ_{max} are displayed in Table 3 along with the description of the experimental absorptions in terms of the dominant one-electron vertical excitations.

The UV–vis absorption spectra measured in solutions show a strong absorption in visible region. Measured λ_{max} are 505 nm (CCl_4), 510 nm (EtOH) and 517 nm (DMSO) respectively. Theoretical calculations for both conformers predict the appearance of a very strong electronic transition in the visible region and give for this excitation larger oscillator strength. The calculated λ_{max} of trans-TR is 535 nm (CCl_4), 544 nm (EtOH) and 546 nm (DMSO). In particular, λ_{max} of trans-TR are larger than that of cis-TR 11 nm (vacuum) and 11 nm (CCl_4), whereas λ_{max} of trans-TR are little smaller than that of cis-TR 3 nm (EtOH) and 4 nm (DMSO). For trans-TR, λ_{max} mainly derives from the excitation HOMO → LUMO (55%), the second contributor to the lowest-energy is HOMO − 1 → LUMO (35%). By reference to Fig. 4, this process can be described as an intramolecular charge-transfer from the naphthyl to phenyl ring. For cis-TR, λ_{max} is also mainly due to the excitation HOMO → LUMO (62%), while, the second contributor to the lowest-energy is both HOMO − 1 → LUMO (15%) and HOMO → LUMO + 1 (15%).

Table 3
Comparison between experimental and theoretical λ_{max} (nm).

Solvent	Experiment	Calculation			
		Trans-TR	Description	Cis-TR	Description
vapor		529 ($f = 0.061$)	H → L, H − 1 → L	518 ($f = 0.089$)	H → L, H − 1 → L, H → L + 1
CCl_4	505	535 ($f = 0.11$)	H → L, H − 1 → L	524 ($f = 0.13$)	H → L, H − 1 → L, H → L + 1
EtOH	510	544 ($f = 0.13$)	H → L, H − 1 → L	547 ($f = 0.11$)	H → L, H − 1 → L, H → L + 1
DMSO	517	546 ($f = 0.14$)	H → L, H − 1 → L	550 ($f = 0.11$)	H → L, H − 1 → L, H → L + 1

Since the experimental results are recorded without consideration of conformers, they are only comparable to a certain degree with the calculated λ_{max}. In addition, TR containing a hydroxyl group which is ortho to the azo group within naphthyl can exist as azo and hydrazone tautomers, with the relative amounts varying with external parameters such as solvent and temperature [30]. Therefore, the electronic structures of TR can be affected strongly by the preferential stabilization of one tautomer over the other, and this may account for some of the differences between the calculation and experiment.

4. Conclusions

In this work, 1-[(4-methyl-2-nitrophenyl)azo]-2-naphthalenol (TR) nanoparticles of 80 nm were obtained by anti-solvent precipitation. The produced TR achieves higher surface charge, more dispersed stability in the medium and good electrophoretic characteristics.

In addition, geometries of trans- and cis- TR were optimized using DFT method at B3LYP/6-31 + G* level. Our calculations demonstrate the planar structure for trans-TR, which is more stable than cis-TR. For both conformers, UV–vis spectra have been predicted with PCM-TD-DFT calculations. The theoretical λ_{max} of both trans- and cis-TR are very similar. In comparison to the experiments, the calculated results give slight red shifted absorption wavelength.

Acknowledgments

This work was supported by National “863” Program of China (No.2008AA03A332 and No. 2009AA033301) and NSFC of China (No.20821004 and No. 20990221).

References

[1] Chen Y, Au J, Kazlas P, Ritenour A. Nature 2003;423:136–7.
[2] Gelinck GH, Huttema HE, Veenendaal E. Nature Materials 2004;3:106–10.
[3] Rogers JA, Bao Z, Baidwin K. Proceedings of the National Academy of Sciences 2001;98:4835–40.
[4] Comiskey B, Albert J, Yoshizawa H. Nature 1998;394:253–5.
[5] Croucher MD, Hair ML. Industrial Engineering Production Research Development 1981;20:324–9.
[6] Werts MPL, Badila M, Brochon C, Hebraud A, Hadziioannou G. Chemistry of Materials 2008;20:1292–8.
[7] Kim MK, Kim CA, Ahn SD, Kang SR, Suh KS. Synthetic Metals 2004;146:197–9.
[8] Nguyen D, Zondanos HS, Farrugia JM, Serelis AK, Such CH, Hawkett BS. Lamgmuir 2008;24:2140–50.
[9] Jihai Duan, Yaqing Feng, Guang Yang, Wenliang Xu, Xianggao Li, Ying Liu, et al. Industrial and Engineering Chemical Research 2009;48:1468–75.
[10] Yu DG, An JH, Bae JY, Ahn SD, Kang SY, Suh KS. Macromolecules 2005;38:7485–91.
[11] Yu DG, An JH, Bae JY, Jung DJ, Kim S, Ahn SK, et al. Chemistry of Materials 2004;16:4693–8.
[12] Fu H, Yao J. Jouranal of the American Chemical Society 2001;123:1434–9.
[13] Gong XC, Milic T, Xu C, Battea JD, Drain CM. Journal of the American Chemical Society 2002;124:14290–1.
[14] An BK, kwon SK, Jung SD, Park SY. Journal of the American Chemical Society 2002;124:14410–5.
[15] Kurita N, Tanaka S, Itoh S. Journal of Physical Chemistry A 2000;104:8114–20.
[16] Fliegl H, Kohn A, Hattig C, Ahlrichs R. Journal of the American Chemical Society 2003;125:9821–7.
[17] Astrand P, Ramanujam PS, Hvilsted S, Bak KL, Sauer SPA. Journal of the American Chemical Society 2000;122:3482–7.

[18] Chung FH. Crystallography of toluidine red. Journal of Applied Crystallography 1971;4:79–80.
[19] Jacquemin D, Preat J, Wathelet V, Fontaine M, Perpete EA. Journal of the American Chemical Society 2006;128:2072–83.
[20] Cossi M, Barone V, Cammi R, Tomasi J. Chemical Physics Letters 1996;255:327–35.
[21] Aguilar MA, Olivares FJ, Tomasi J. Journal of Chemical Physics 1993;98:7375–84.
[22] Cossi M, Barone V, Mennucci B, Tomasi J. Chemical Physics Letters 1998;286:253–60.
[23] Preat J, Jacquemin D, walthelet V, Andre JM, Perpete EA. Journal of Physical Chemistry A 2006;110:8144–50.
[24] Casda ME, Jamorski C, Casida KC, Salahub DR. Journal of Chemical Physics 1998;108:4439–49.
[25] Stratmann RE, Scuseria GE, Frisch MJ. Journal of Chemical Physics 1998;109:8218–24.
[26] Cossi M, Barone V. Journal of Chemical Physics 2001;115:4708–17.
[27] Guillemoles J-F, Barone V, Joubert L, Admo C. Journal of Chemical Physics 2002;106:11354–60.
[28] Cave RJ, Edward W, Castner Jr . Journal of Chemical Physics 2002;106:12117–23.
[29] Abbott LC, Batchelor SN, Oakes J. Journal of Physical Chemistry A 2005;109:2894–905.
[30] Snehalatha M, Ravikumar C, Hubert I. Solid State Sciences 2009;11:1275–82.